Geologica Acta, Vol.16, Nº 4, December 2018, 357-373
DOI: 10.1344/GeologicaActa2018.16.4.2
© P. Granado, S. Tavani, N. Carrera, J.A. Muñoz, 2018 CC BY-SA

geologica acta

Deformation pattern around the Conejera fault blocks (Asturian Basin, North Iberian Margin)

P. GRANADO[1] S. TAVANI[2] N. CARRERA[1] J.A. MUÑOZ[1]

[1]Institut de Recerca Geomodels, Departament de Ciències de la Terra i de l'Oceà, Universitat de Barcelona
C/ Martí i Franquès s/n, 08028 Barcelona. E-mail: pablomartinez_granado@ub.edu

[2]Dipartimento di Scienze della Terra, dell'Ambiente e delle Risorse (DISTAR), Università degli Studi di Napoli Federico II
Via Cupa Nuova Cintia, 21, 80126, Napoli, Italy

ABSTRACT

The Asturian Basin is located on the coastline of the North Iberian Margin. This basin is dissected by long-lived E-, NE- and NW-striking faults that delineate a series of extensional fault blocks that became shortened during the Upper Cretaceous to Cenozoic Alpine convergence. In the Conejera cove, the NE-striking and SE-dipping Conejera Fault displays a remarkable example of contractional deformation, promoted by the mechanical contrast within the Lower to Middle Jurassic stratigraphic series. Field observations and structural analysis carried out in this study reveal: i) a first system of orthogonal cross-joints oblique to the Conejera Fault and other major onshore boundary faults, ii) a second system of meso-extensional faults parallel to the Conejera Fault, and developed by the reactivation and linkage of the orthogonal cross-joints and iii) a series of contractional folds, thrusts and pressure solution with a predominant NE to ENE trend. Observed relationships and structural analysis suggest an obliquity between the here inferred direction of the Late Jurassic-Early Cretaceous stretching (*i.e.* about N015E) and the onshore boundary faults, whereas the contractional structures are broadly parallel to the NE-striking Conejera Fault and suggest a roughly SSE- to SE-oriented Alpine convergence.

KEYWORDS | **Asturian Basin. Conejera Fault blocks. Deformation patterns. Reactivation. North Iberian Margin.**

INTRODUCTION

Since the early reference work of Gillcrist *et al.* (1987), many studies have documented how inheritances exert a strong control on subsequent deformation stages (*e.g.* Cooper and Williams, 1989; Coward *et al.*, 1989, 1991; Butler *et al.*, 2006; Frizon de Lamotte *et al.*, 2009). Great attention has been dedicated to the role played by inherited fault networks (*e.g.* De Gracianski *et al.*, 1989; Thomas and Coward, 1995; Tavarnelli, 1996; Macedo and Marshack, 1999; Carrera *et al.*, 2006; Henza *et al.*, 2011; Tavani *et al.*, 2013; Tavani and Granado, 2015; Granado *et al.*, 2016) or the rheological properties (*e.g.* Hillis, 1956; Davis and Engelder, 1985; White *et al.*, 1986; Boyer, 1995; Butler *et al.*, 2006) at all scales of observation. In this sense, the reactivation and/or linkage of previous mesostructures is also commonly observed during the transition from one tectonic regime to the subsequent ones (*e.g.* Engelder and Geiser, 1980; Dyer, 1988; Olson and Pollard, 1989; Cruikshank *et al.*, 1991; Willemse *et al.*, 1997; Wilkins *et al.*, 2001; Silliphant *et al.*, 2002; Graham Wall *et al.*, 2003; Bergbauer and Pollard, 2004; Crider and Peacock, 2004; Myers and Aydin, 2004; Agosta and Aydin, 2006; Blenkinsop, 2008; Brogi, 2011; Tavani *et al.*, 2011a, b). A key observation arising from these studies is that the relationship between the stress field and the mesostructural deformation pattern can be assessed in the presence of previously-developed mesostructures. Accordingly,

defining the relationships between different mesostructures such as folds and fractures (*i.e.* including joints, faulted joints, faults, veins and pressure solution seams) in poly-deformed rocks is a powerful tool to decipher the tectonic history of an area.

The outcrop presented in this study has been described in detail by Uzkeda *et al.* (2013) in terms of its geometries and broad kinematics. Our aim is to complement their study by providing further evidence of structural development arising from detailed mesostructural analysis of the Conejera Fault blocks. Insights into the extensional history of the studied section have been gained and compared with other coetaneous Late Jurassic-Early Cretaceous extensional basins also incorporated in the Pyrenean orogeny and related Iberian intraplate belts. Throughout the manuscript, the terminology proposed by Butler (1989), McClay (1989, 1995) and Williams *et al.* (1989) will be used when referring to the structural styles related to inversion tectonics.

GEOLOGICAL SETTING

The E–W-elongated Asturian Basin is a Late Jurassic-Early Cretaceous extensional basin of the North Iberian Margin whose southernmost part crops out in Asturias (Fig. 1A). Filled by thick Permian to Mesozoic successions, it is bounded and dissected by E-, NE- and NW-striking faults, most of them involving the underlying Variscan basement (Lepvrier and Martínez-García, 1990). The larger onshore faults are the E-striking Llanera and Ribadesella faults, the long NW-striking Ventaniella Fault, and a series of shorter NE-striking faults such as the Villaviciosa Fault (Fig. 1A), amongst others. The Asturian Basin formed during the predominant extensional tectonic regime that affected the Iberian plate and the North Atlantic, from the late Carboniferous collapse of the Variscan orogen until the onset of Late Cretaceous convergence between Eurasia-Africa (Arthaud and Matte, 1977; Dallmeyer and Martínez-García, 1990; Lepvrier and Martínez-García, 1990). Onset of rifting is recorded by fault-bound sedimentation during Stephanian-Permian (Dallmeyer and Martínez-García, 1990; Lepvrier and Martínez-García, 1990). Rifting renewed during a second and main Late Jurassic-Early Cretaceous rifting episode, culminating with the opening of the Bay of Biscay (Sibuet *et al.*, 1971, 2007; Arthaud and Matte, 1977; Boillot, 1984; Dallmeyer and Martínez-García, 1990; Lepvrier and Martínez-García, 1990; Ferrer *et al.*, 2008; Roca *et al.*, 2011; Grobe *et al.*, 2014; Tugend *et al.*, 2014; Cadenas *et al.*, 2017). These two rifting events were separated by a period of relative quiescence with sedimentation spanning from Late Triassic to Middle Jurassic, characterised by the onset of evaporitic tidal flats and carbonate ramps (Valenzuela *et al.*, 1986; Barrón *et al.*, 2006). Docking of the Iberian and Eurasian plates during the Late Cretaceous to Cenozoic deformed and uplifted the North Iberian Margin by the reactivation of the major bounding faults (Lepvrier and Martínez-García, 1990; Alonso *et al.*, 1996, 2007; Álvarez-Marrón *et al.*, 1996; Gallastegui *et al.*, 1997; Gallastegui, 2000; Muñoz, 2002; Roca *et al.*, 2011; Carola *et al.*, 2013). As a result, the Asturian Basin was inverted (Uzkeda *et al.*, 2016) with the Mesozoic cover remaining largely attached to its autochthonous Variscan basement (Pulgar *et al.*, 1999). Unconformities found in Late Cretaceous-Paleocene and Middle Eocene sediments, as well as post lower Oligocene sediments preserved in the footwall of basement thrust slices evidence the thick-skinned deformation of the Asturian Basin in both the offshore and onshore domains (Boillot *et al.*, 1979; Alonso *et al.*, 1996; Álvarez-Marrón *et al.*, 1996; Riaza-Molina, 1996; Pulgar *et al.*, 1999; De Vicente *et al.*, 2007).

THE CONEJERA FAULT BLOCKS

Stratigraphy and brief structural description

The Conejera cove locates East of the village of Tazones and the Villaviciosa estuary (Fig. 1B). Along the studied section, the rocks exposed consist of well-bedded nodular limestones and alternating marls and limestones belonging to the pre-rift Lower to Middle Jurassic (late Sinemurian to early Bajocian) Rodiles Formation (Fm.) (Figs. 2; 3). The Rodiles Fm. has been subdivided into the Buerres and the Santa Mera members (mbs.) (Suárez-Vega, 1974; Valenzuela *et al.*, 1986). The Buerres Member (Mb.) is constituted by nodular limestones with interlayered limestone beds and marls arranged in decimetre to metre-thick beds, deposited in a shallow carbonate ramp; the Santa Mera Mb. is made up of limestones and marls in rhythmically-arranged centimetric to decimetric planar-parallel beds, deposited in a restricted carbonate ramp to open shelf environment (Valenzuela *et al.*, 1986; Robles *et al.*, 2004). Unconformably above, the Upper Jurassic Kimmeridgian units of the La Ñora Fm. (Suárez-Vega, 1974; Valenzuela *et al.*, 1986; Schudack and Schudack, 2002) were regionally deposited, but are poorly exposed above the Conejera cove cliffs (Pignatelli *et al.*, 1973, Fig. 1B). This formation consists of conglomerates, sandstones and clays deposited in alluvial fans and valley infills (Fig. 3) deposited at the onset of the Upper Jurassic-Lower Cretaceous rifting (Valenzuela *et al.*, 1986; Lepvrier and Martínez-García, 1990).

The Conejera Fault is in close proximity to the larger basement-involved Villaviciosa Fault (Fig. 1A). The Conejera Fault dips to the SE and is parallel to the NE-striking basement-involved fault system of the Asturian

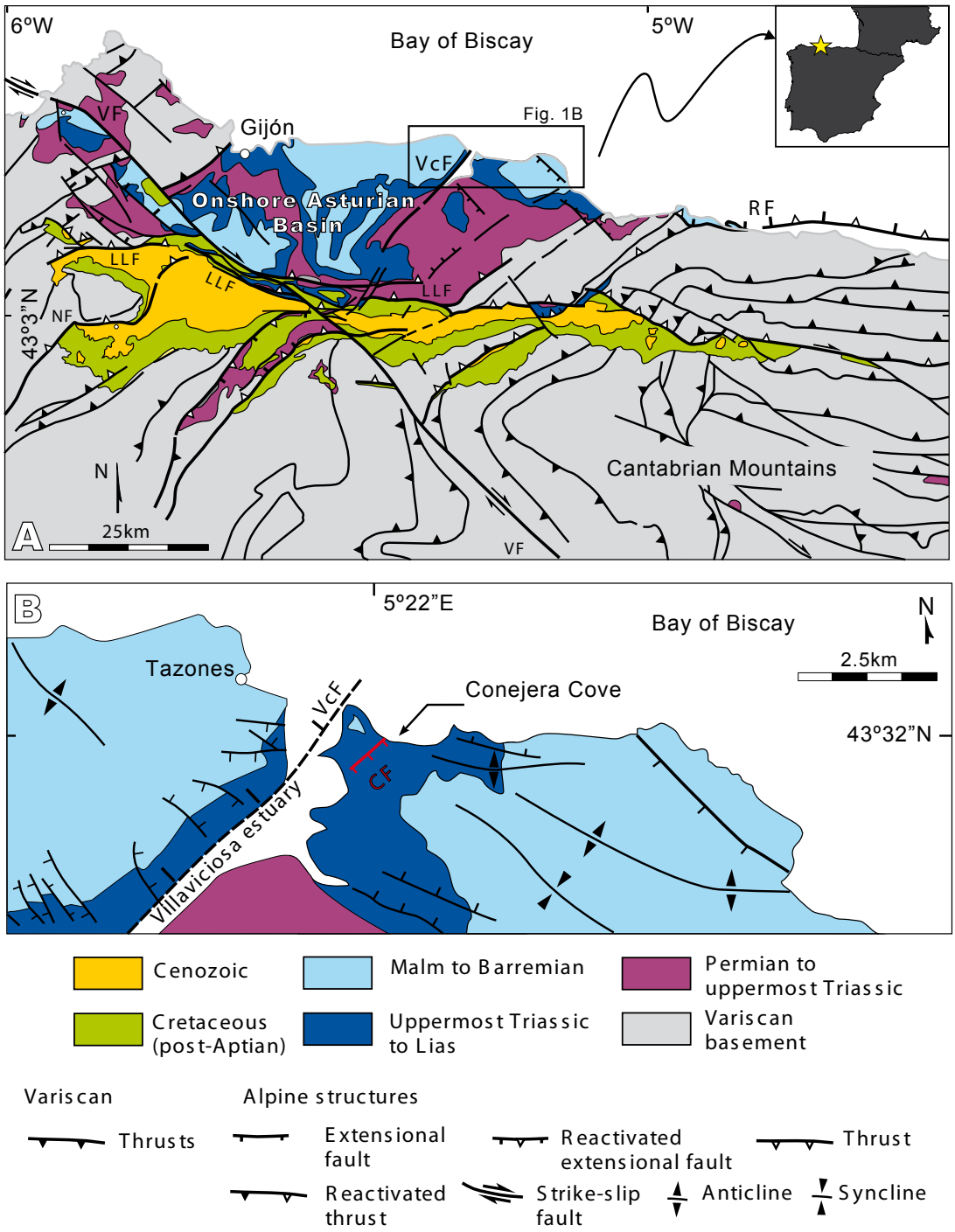

FIGURE 1. A) Geological map of the onshore Asturian Basin. LLF: Llanera Fault; NF: Naranco Fault; RF: Ribadesella Fault; VcF: Villaviciosa Fault; VF: Ventaniella Fault. Modified from Lepvrier and Martínez-García (1990) and Pulgar *et al.* (1999). B) Geological map of the study area. CF: Conejera Fault. Modified from Pignatelli *et al.* (1973).

Basin (Lepvrier and Martínez-García, 1990). The Conejera Fault is most likely detached along the shallow Rhaetian-Hettangian evaporites of the Gijón Fm. (Uzkeda *et al.*, 2013), but may have been kinematically linked to a basement fault striking parallel; this is the structural style found in the offshore region (Zamora *et al.*, 2017). Although its hanging-wall displays a significant shortening, the Conejera Fault presents an extensional fault offset, juxtaposing the upper member of the Rodiles Fm. above its lower member (Fig. 2). This indicates that the Conejera Fault was either not inverted or only mildly inverted during the Alpine convergence, since the null point (Williams *et al.*,

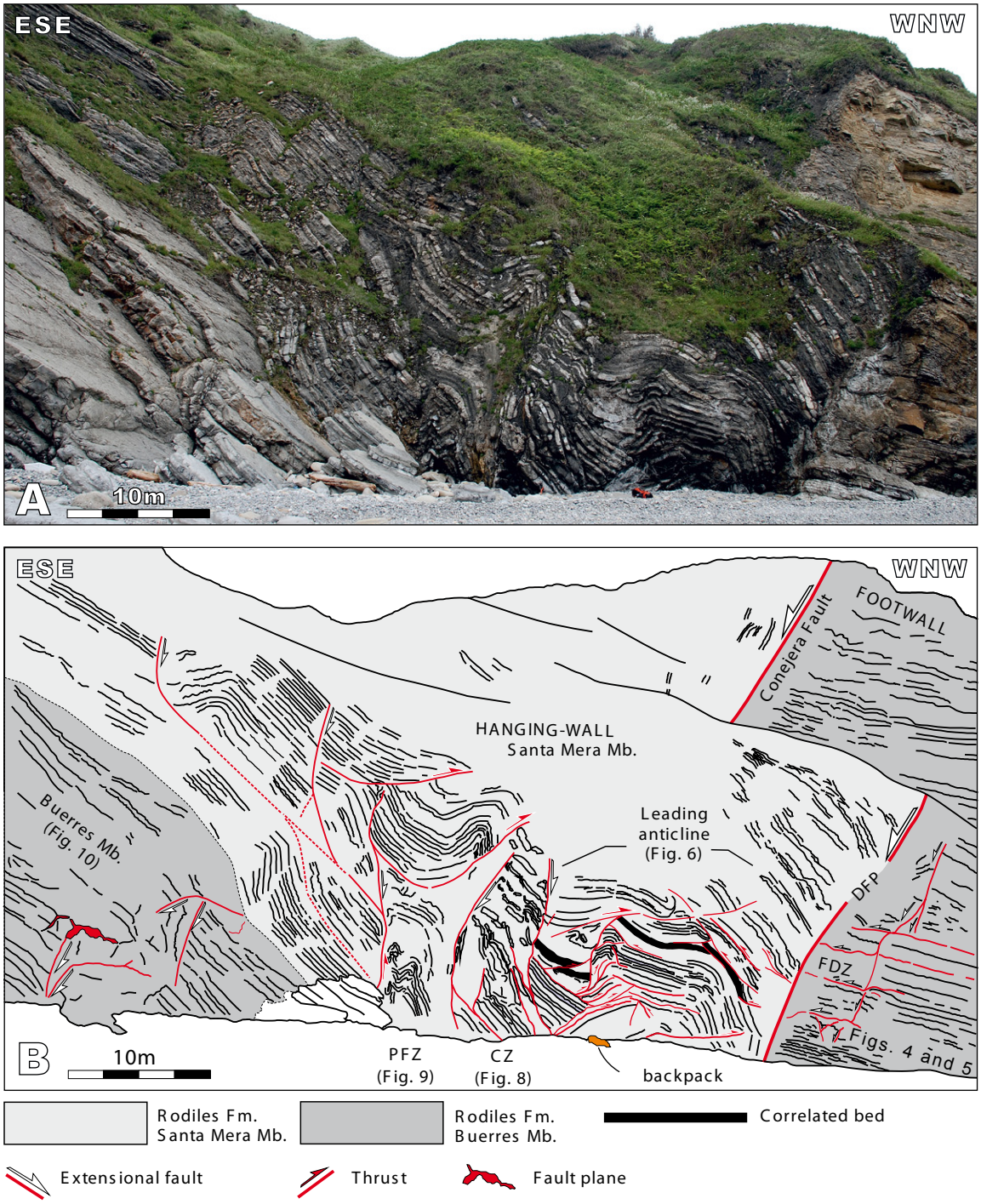

FIGURE 2. The studied Conejera Fault blocks at Conejera cove. A) On the hanging-wall (left) younger units are juxtaposed to older units on the footwall (right), indicating an extensional offset of the Conejera Fault. Orange backpack at centre right on gravel beach for scale. B) Photo interpretation. The outcrop has been divided according to the deformation patterns related to the mechanical stratigraphy. CZ: Central Zone; PFZ: Pseudo-flower Zone sensu McClay (1989). DFP: Discrete Fault Plane; FDZ: Footwall Damage Zone. Google Earth outcrop coordinates: 43º31'57"N and 5º21'53"W.

1989; Turner and Williams, 2004), if at all present, would be located above the fault plane outcrops. In the hanging-wall and the footwall of the Conejera Fault, the Rodiles Fm. shows evidences of intense contractional deformation represented by reactivated extensional faults, tight folds and thrusts, and pressure solution seams. This deformation decreases away from the fault (*i.e.* in a buttressing deformation gradient; Fig. 2) but is significantly controlled by the different layering and mechanical properties of the Buerres and the Santa Mera mbs. The lower member is

much less influenced by the layering that the upper one, in which the marl and organic shale interbeds behave as effective detachment layers. In the following sections, the outcropping Conejera Fault blocks and the observed structures are described and analysed in detail.

The Conejera Fault

The outcropping Conejera Fault dips about 55º to the SE (Fig. 4A, B). It consists of 5–40cm-thick fault core of carbonate breccias enclosed in a fault gouge made up of strongly smeared marls with a fault-parallel fabric. The upper boundary of these fault rocks is a discrete planar surface of constant strike and dip (Fig. 4B), whereas the lower one is a rather irregular surface.

Footwall deformation

The footwall of the Conejera Fault is characterized by a 3–4m-thick damage zone. The upper boundary of the damage zone is well defined by the base of the fault core breccias, whereas the lower boundary is diffuse, and defined by the progressive disappearance of the fault-related deformation (Fig. 5). However, a set of trough-going extensional faults parallel to the Conejera Fault delimit a volume of substantially strained rocks (Fig. 4); away from these faults, strain progressively diminishes. In the damage zone, most of the fractures are synthetic to the Conejera Fault, but also some antithetic fractures are present (Figs. 4C; 5). In the footwall to the Conejera Fault, beds of the Buerres Mb. display a constant dip of about 25º to the NW. Widespread pressure solution seams are parallel to bedding (Fig. 5C, D) and most likely related to burial. Within the damage zone, bedding shows a top-to-the SE bed-parallel slip along the contacts between the limestone layers, and flow along the marl beds (Figs. 4; 5). This layer-parallel motion is related to the extensional displacement of the Conejera Fault, accommodated through a wide fault zone as reported for other rift settings (*e.g.* Jackson *et al.*, 2006; Wilson *et al.*, 2009).

Apart of this deformation, the footwall rocks close to the Conejera Fault appear deformed by joints and small displacement faults; additional pressure solution seams are also present, and strike at high angles to bedding. The small displacement faults (*i.e.* mesofaults) abut against or sole along bed boundaries, and consistently show extensional displacements in the order of centimetres-decimetres (Fig. 5A, C). These mesofaults are steeply-dipping, trend NE-SW and dip in the same and the opposite senses to the Conejera Fault (Fig. 4C) at 60–70º to bedding (Fig. 5). In fact, these mesofaults define a conjugate fault system, having their acute dihedral angle broadly perpendicular to bedding. Despite the observed offsets, most of these mesofaults display a tooth-shaped cross-sectional geometry

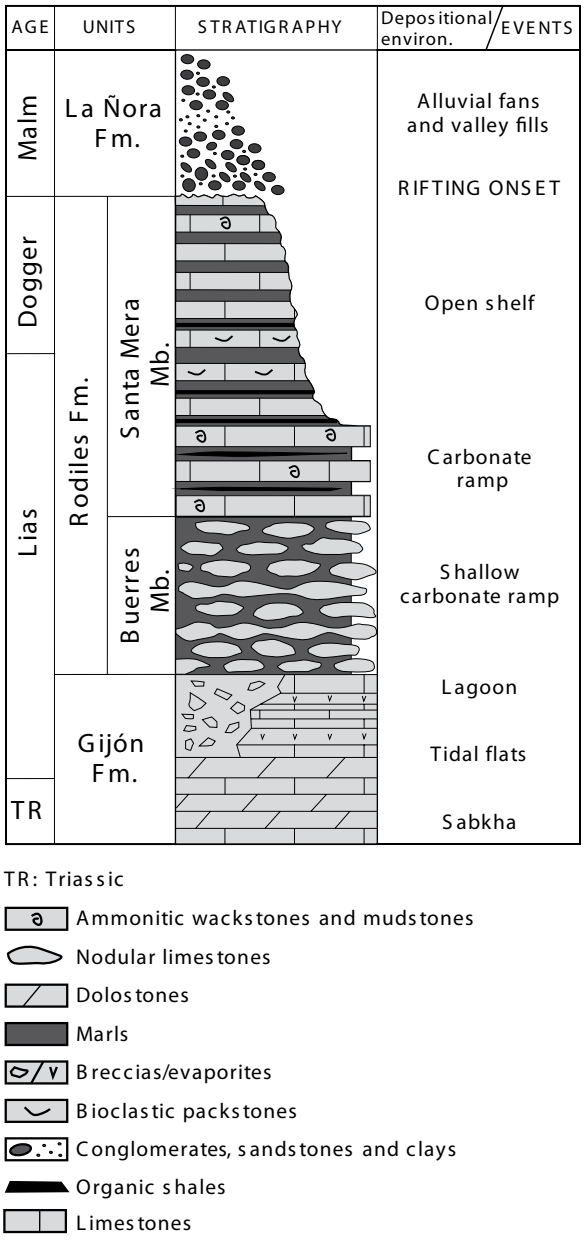

FIGURE 3. Simplified stratigraphic column, depositional environments and main events for the Late Triassic-Middle Jurassic pre-rift and Late Jurassic syn-rift units of the onshore part of the Asturian Basin. Modified from Valenzuela *et al.* (1986), Robles *et al.* (2004) and Barrón *et al.* (2006).

(Fig. 5C), indicating their reactivation as pressure solution planes. Additional pressure solution seems strike almost perpendicular to bedding. These features are indicative of layer parallel-shortening, post-dating the extensional kinematics of the Conejera Fault.

Hanging-wall deformation

The hanging-wall block has been divided into several deformation domains in order to ease its description and

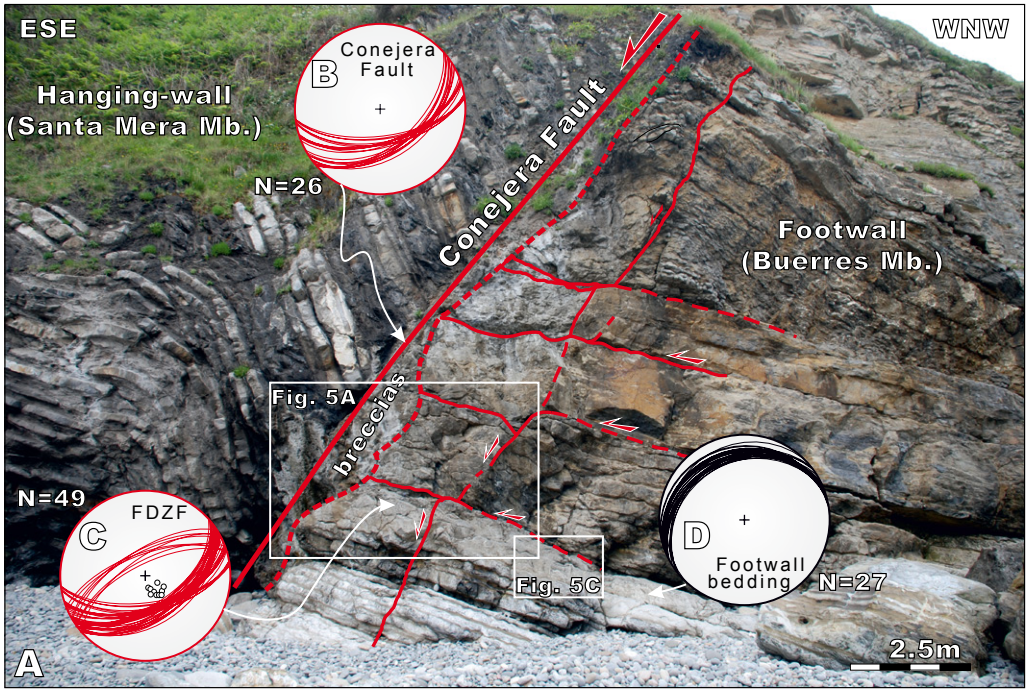

FIGURE 4. A) The Conejera Fault and its adjacent footwall block. B) Great circles to the Conejera Fault discrete plane. C) Great circles to the footwall Fault Damage Zone Faults (FDZF), and poles to bedding. D) Great circles to the attitude of the footwall beds. All projections lower hemisphere equal area stereoplots.

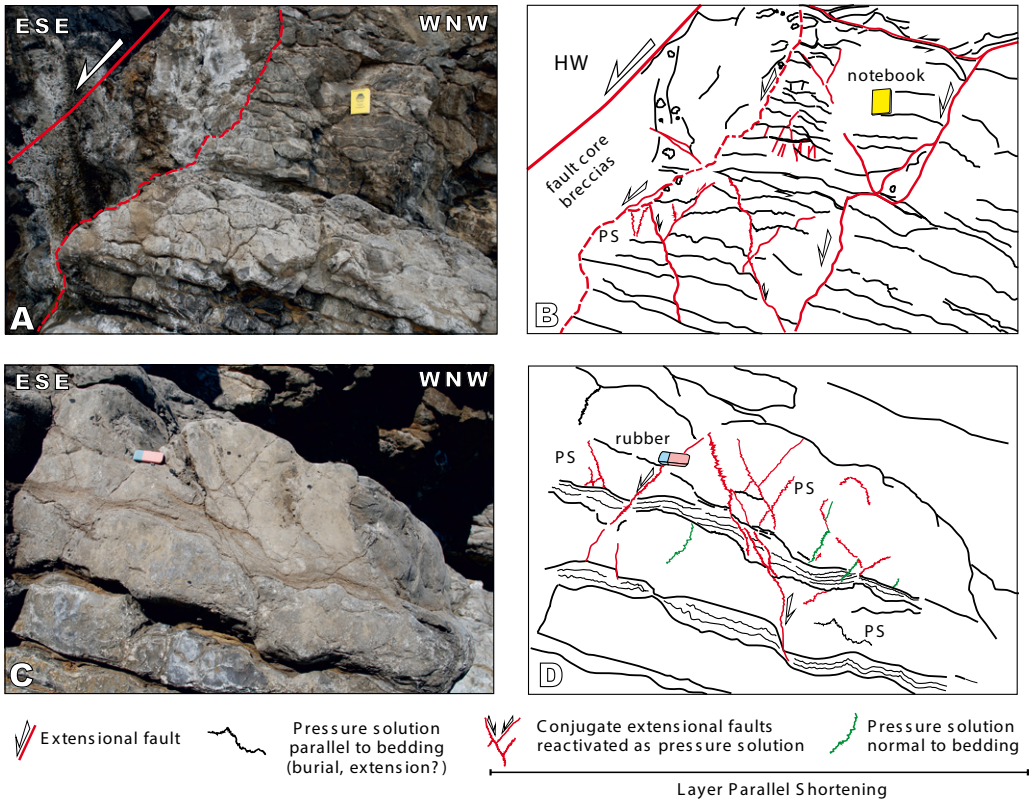

FIGURE 5. Footwall mesostructures. A) Detailed photo of the Conejera Fault (i.e. discrete plane and breccia fault rock) and adjoining footwall fault damage zone. B) Photo interpretation showing the main features of the footwall damage zone deformation. C) Close up photo of footwall damage zone deformation in a zone that is further away of the fault. D) Photo interpretation denoting how the conjugate extensional faults reactivated as Pressure Solution (PS) surfaces upon shortening. Field notebook and rubber for scale. See Figure 4 for photo location.

interpretation. The subdivision takes into account the mechanical stratigraphy of the two members of the Rodiles Fm., the observed structural styles, and the contractional deformation gradient (Fig. 2B). In this sense, the deformation gradient increases towards the Conejera Fault, but it is also directly related to the mechanical stratigraphy involved. The Santa Mera Mb. attained most of the observable contractional strain and is partially detached from the underlying Buerres Mb. by thin-skinned thrusts (Fig. 2). On the other hand, the Buerres Mb. is affected by steeply-dipping extensional faults and well-developed joints, but is devoid of any significant compressional mesostructures. According to the structural styles and deformation gradient, the Santa Mera Mb. deformation has been subdivided as follows: a leading anticline, directly juxtaposed to the Conejera Fault, a central zone, and a pseudo-flower zone (*sensu* McClay, 1989, 1995). The underlying Buerres Mb. outcrops at the hanging-wall's trailing edge. All these zones are analysed in depth in the following sections.

Santa Mera Mb. deformation

Leading anticline

This is the leading zone of contractional deformation of the Conejera hanging-wall block (Fig. 6). It is characterized by a complex mesostructural deformation pattern which includes: reactivated extensional faults, thrusts, joints, foliations, folds, pressure solution seams and carbonate-filled veins. Tectonic thinning and thickening of beds is common in this structural domain and has been taken into account during tentative bed correlations (Fig. 2B). Despite the structural complications, the broad bedding attitude describes a NE-striking and NW-verging anticline (Fig. 6). Its forelimb dips steeper to the NW and its lower parts consist of two bedding panels divided by a SE-dipping axial surface, which is broadly parallel to the Conejera Fault. However, the forelimb of the leading anticline is affected by several SE-directed backthrusts that nucleate at the Conejera Fault and propagated upward into the hanging-

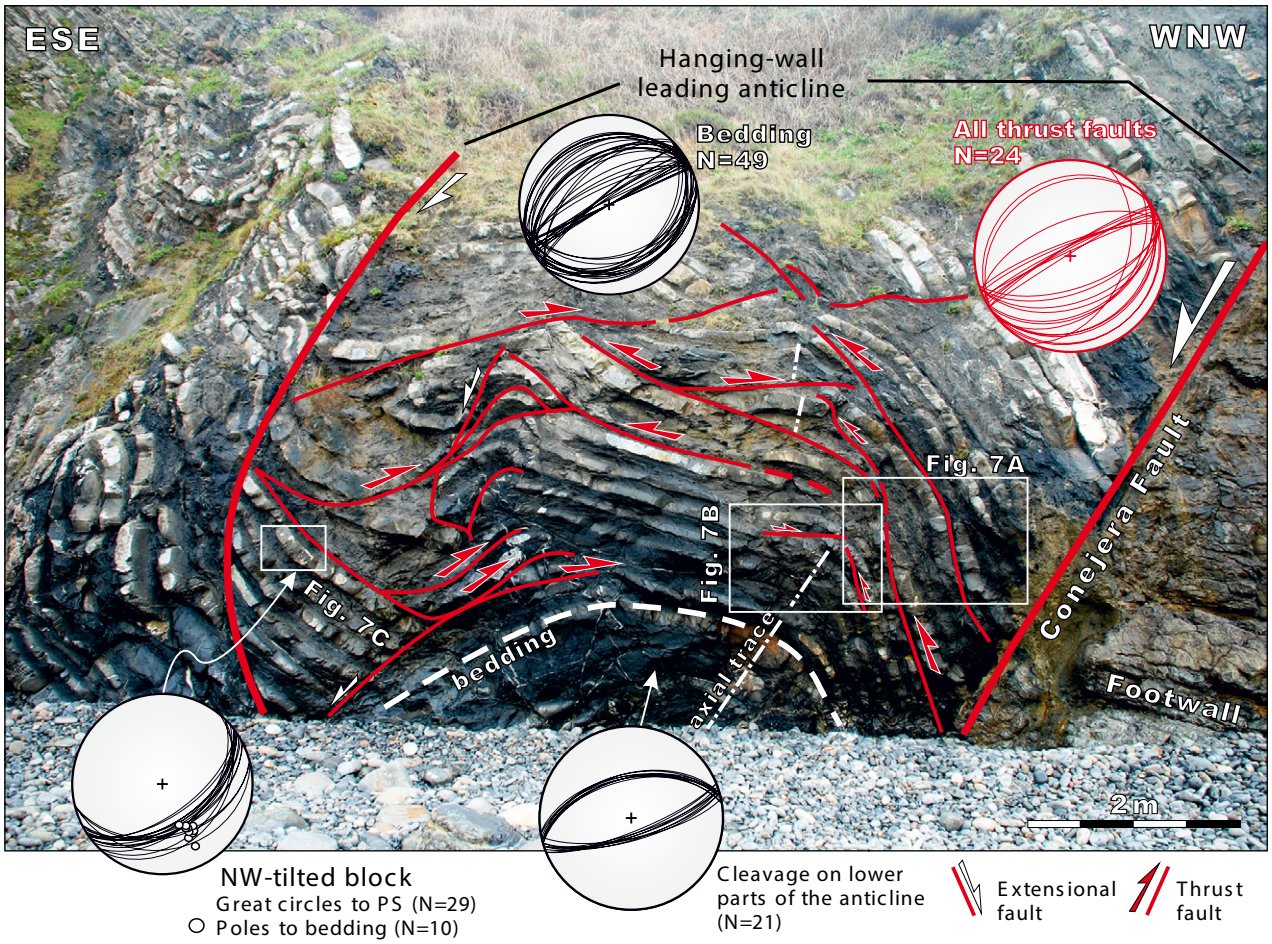

FIGURE 6. Interpreted photo of the Conejera Fault hanging-wall leading anticline. Stereoplots are provided for the bedding attitude, the Conejera Fault, the buttressing-related thrusts, and pressure solution cleavages. All projections are lower hemisphere equal area stereoplots. See Figure 2 for location.

wall along the marl beds (Figs. 6; 7A). Carbonate veins occur parallel to the sheared marl horizons interlayered between the mud limestone beds, thus, defining the location of slip surfaces, and indicating fluid circulation during shortening. These faults show displacements in the order of few meters, accommodating space problems developed during tightening of the structure. Some of these thrusts in fact displace and post-date the SE-dipping axial surface (Fig. 6). In the anticline hinge, single-layer triangle zones are also present (Fig. 7B).

The southeastern limb (*i.e.* backlimb) of the leading anticline is also affected by small-displacement thrusts that offset both bedding and upright faults and form a thrust stack of carbonate beds (Fig. 6). However, bed correlations in this sector still indicate the presence of extensional offsets (Fig. 2B). A fault-bounded block preserving relatively 'undisturbed' bedding can be recognised. Bedding within this block dips about 50º to the NW (*i.e.* toward the Conejera Fault) and is bounded by two faults with *ca.* 60º cut-off angles (Fig. 6). This isolated fault-bound block displays a well-developed pressure solution cleavage perpendicular to the limestone beds (Fig. 7C); the pressure solution seams abut against the marl interlayers, which in turn display a strong bed-parallel fabric. As shown by the plotted mesostructural data, the orientation of the pressure solution seams roughly strikes parallel to the Conejera Fault and the central zone faults (Figs. 2; 8). In the lower reaches of the leading anticline, cleavages strike ENE-WSW, sub-parallel to the Conejera Fault (Fig. 6).

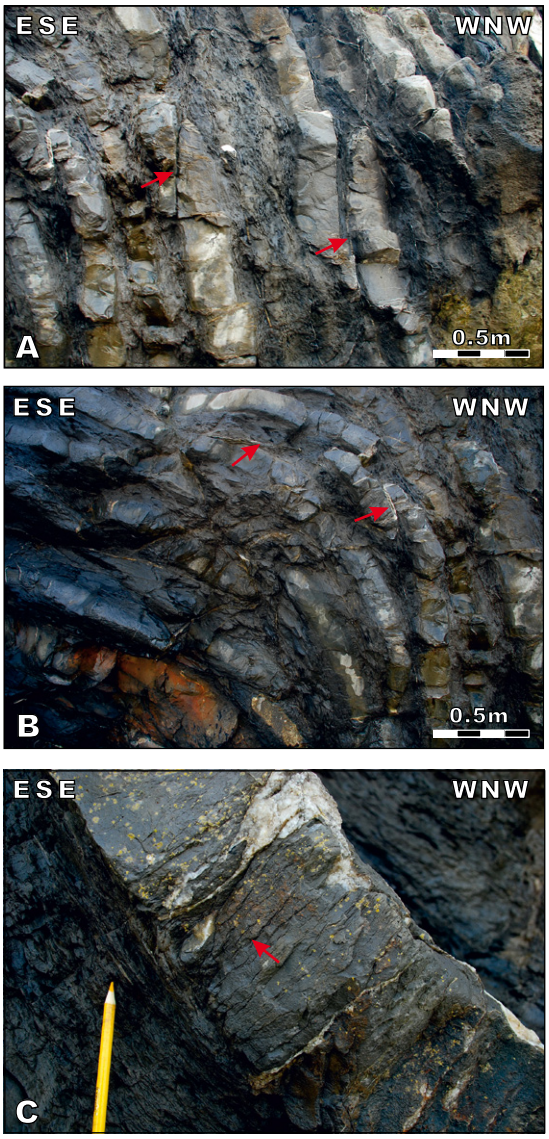

FIGURE 7. Detailed photos of the thrusts and pressure solution cleavage present in the leading anticline of the Conejera Fault hanging-wall. A) Upright low-angle to bedding SE-directed thrusts. B) Triangle zone of bedding-detached thrusts. C) Normal to bedding pressure solution seams; pencil for scale. See Figure 6 for location.

Central Zone (CZ)

The Central Zone is limited by two concave-to-the NW faults (Fig. 8A, B). These two faults bound a zone of NW-dipping and partially dismembered limestone and marl beds. In the upper parts of these concave faults, bedding dips in opposite direction, whereas in their lower reaches bedding dips towards the same direction as the faults. The origin of these structures is analysed in the following sections.

'Pseudo-flower' Zone

This zone is bound by the CZ to the NW, and extends to the SE, including a series of compressional and extensional features. The extensional features are represented by two extensional faults displaying a ramp-flat-ramp geometry (Fig. 2) within the Santa Mera Mb. Across these extensional faults, dark shale layers become thicker and more abundant towards the Conejera Fault. These two extensional faults seem to branch downwards into a single steeply-dipping to overturned extensional fault within the Buerres Mb. (Figs. 2; 9). In addition, several thrusts occur within the Santa Mera Mb. shale layers, internally detaching it, and overall, decoupling the contractional deformation from the underlying Buerres Mb. (Figs. 2; 9). In the lower reaches of the outcrop (Fig. 9B), a steeply-dipping to upright fault displays an apparent reverse slip. No striations along the fault surface have been found to properly constrain its kinematics but the associated cut-off angles and drag folds are indicative of an extensional origin. A SE-directed thrust has a thrust-related anticline affecting strongly folded and broken up limestone and marl beds, whereas in the upper reaches, several thrusts propagate along the shale layers. In fact, the lower extensional fault is by-passed by the SE-directed thrust mentioned above (*i.e.* a by-pass back-thrust *sensu* McClay, 1989, 1995). Above these structures,

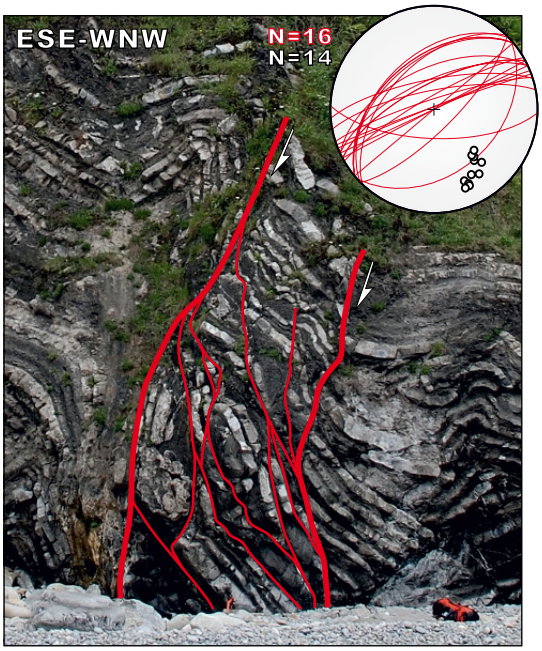

FIGURE 8. The structure of the Central Zone (CZ) consists of two major concave-to-the-NW extensional faults (thick red lines) bounding a series of faulted and dismembered NW-dipping beds. Backpack on the gravel beach for scale. See Figure 2 for location. Lower hemisphere equal area projection of great circles to faults and poles to bedding.

incompetent beds of the Santa Mera Mb. tighten upwards into a NW-directed thrust-related anticline (Fig. 9A). This upper anticline and its associated syncline at the rear are also cut by other NW-directed thrust (*i.e.* a hanging-wall directed thrust) with an associated fault-propagation fold.

Buerres Mb. deformation

Beneath and SE of the Pseudo-flower Zone, the Buerres Mb. layers (Figs. 2; 10) dip into the Conejera Fault, and are devoid of any significant contractional mesostructures; no compressional cleavage has been found throughout these dipping layers. Hence, it is an excellent area to investigate the local pre-shortening deformation pattern. In this part of the hanging-wall, extensional fault zones outcrop on well exposed NW-dipping panels. These upright faults are NE-striking, and affect a rather massive carbonate sequence with thin interbedded layers of marls. Although these faults are steeply-dipping to upright, offset of beds and associated fault drag are unequivocally extensional, with development of hanging-wall synclines, footwall anticlines, and breached monoclines, accompanied by bed thinning and stretching along fault zones and around the fault-tip regions (*e.g.* Schlische, 1995; Hardy and McClay, 1999; Fig. 10A, B). Their cut-off angles to bedding are remarkably high (*i.e.* above 60º) and no significant tilting of beds is observed away from the dragged areas.

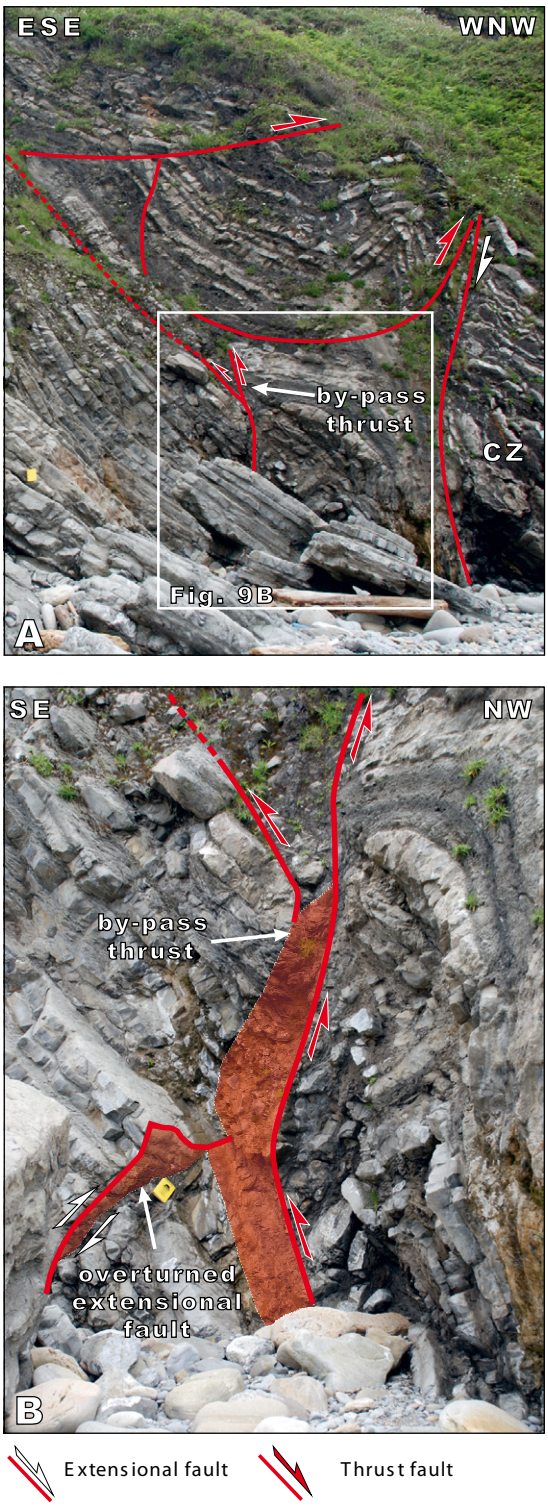

FIGURE 9. Pictures of the Conejera Fault hanging-wall pseudo-flower. The structure is bound to the NW by the concave-to-the NW extensional fault of the Central Zone (Fig. 8) and to the SE by a basal SE-directed back-thrust. The pseudo-flower is constituted by a series of NW- and SE-directed thrusts and open to tight folds detached in the marl and organic rich layers. A) General view of the outcrop. B) Detail of the SE-directed by-pass thrust, and a rotated extensional fault located in its footwall that affects the Buerres Mb. Yellow notebook for scale. For location, see respectively Figures 2 and 9A.

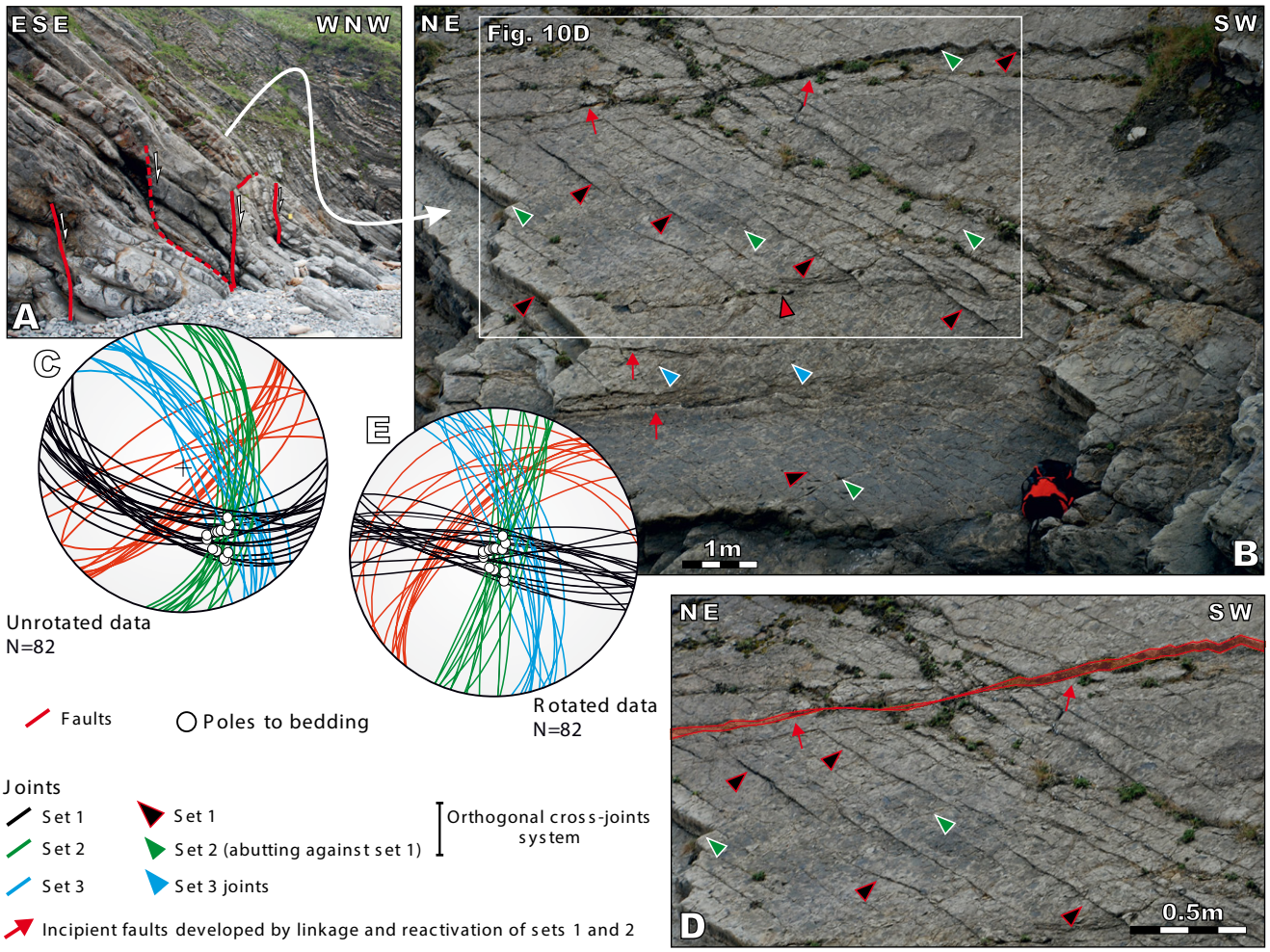

FIGURE 10. Structure of the Buerres Mb. in the Conejera Fault hanging-wall. A) Cross-section view along the southeast part of the Conejera cove outcrop showing the general structure of the Buerres Mb. limestones and their relationship with the overlying Santa Mera Mb. layers. Yellow notebook for scale. B) Frontal view of a of a Buerres Mb. limestone bedding surface showing 3 joint sets, some incipient extensional faults and the drape folds developed over one of the larger extensional faults outlined in Figure 10A; C) Stereoplot with the present day orientation of joints (black, green and blue great circles), faults (red great circles) and poles to bedding. D) Detail of the orthogonal cross-joint system, with a mesofault developed by linkage and reactivation these joints. E) Stereoplot with the orientation of joints and faults once bedding is restored to the horizontal. All projections are lower hemisphere equal area stereoplots.

The NW-dipping layers of the Buerres Mb. also show a well-developed network of joints and incipient faults (Fig. 10B). This fault-fracture network is constituted by: three joint sets striking ESE-WNW, N-S and NW-SE (*i.e.* hereafter referred to as sets 1, 2 and 3, respectively; see Fig. 10B, C), along with the above-mentioned set of NE-striking faults. The mesostructural fracture pattern formed by joint sets 1, 2 and 3 is not straightforward to recognise as a limited deviation from near mutual perpendicularity can be observed on the stereoplot (Fig. 10C). In outcrop, set 1 is the best developed, with longer thoroughgoing joints (*i.e.* systematic set), whereas joints belonging to sets 2 and 3 commonly abut against set 1 (*i.e.* cross-joint sets). In fact, sets 1 and 2 are also perpendicular to bedding as it can be appreciated in the stereoplot projection depicted in Figure 10C, (*i.e.* poles to bedding lie on the joints' big circles intersection). The pattern displayed by bedding and the joint sets 1 and 2 gives place to an orthogonal cross-joint assemblage (*e.g.* Gross, 1993; Bai *et al.*, 2002). In addition, joints belonging to set 1 have attained some vertical displacement that dies out at their tips (Fig. 10D). Joints belonging to set 3 are at high angles to bedding, but slightly deviate from near mutual perpendicularity with set 1.

To further investigate the observed mesostructural pattern, bedding along with the four fracture sets has been restored to its pre-extension and pre-shortening attitude by rotating the NW-dipping bedding (along with the fractures) back to the horizontal (Fig. 10E). Once bedding is restored, joint sets 1 and 2 become upright, normal to bedding, and clearly mutually perpendicular (Fig. 10E). Set 1 becomes ESE-striking (*i.e.* striking about N100E), whereas set 2

becomes NNE-striking (*i.e.* striking about N015E). On the other hand, set 3 joints become NNW-striking and steeply ENE-dipping, and not perpendicular to bedding. Faults become NE-striking, NW-dipping, and oblique to all joint sets. These joints are folded over the hanging-wall synclines and footwall anticlines associated to these NE-striking extensional faults, providing key relative-timing constraints. A proposed origin for the described fracture pattern is addressed in the following section.

DISCUSSION

Extensional kinematics of the Conejera Fault blocks

Lack of a well-developed suite of fault zone striations or any fault structures with kinematic meaning hampers proper assessment of the Conejera Fault kinematics. However, we have been able to broadly differentiate two deformation episodes from the mesostructural deformation pattern of the Conejera Fault and related hanging-wall and footwall blocks (Fig. 11). The observed deformation pattern corresponds to that of an extensional fault whose hanging-wall and footwall have undergone compressional deformation. But once the post-extensional deformation is removed, several key features can be highlighted. In the footwall, we have found evidence of the development of a fault-damage zone, including pressure solution seams parallel to bedding, conjugate extensional faults and bed-parallel shearing; both are consistent with a vertical principal stress: the first probably related to burial, and the last two associated with extensional kinematics. In the hanging-wall, the steeply-dipping to overturned, and the concave-to-the NW faults, become oppositely-dipping to the Conejera Fault and display a clear extensional offset upon restoration. Similar structural styles and kinematics have been defined in other inverted rift settings (McClay *et al.*, 1989; Carrera *et al.*, 2006) and in sandbox analogue models of positive basin inversion (McClay, 1989, 1995; Granado *et al.*, 2017). The geometry of the exposed hanging-wall extensional faults corresponds to a ramp-flat-ramp style; minor changes in the stratigraphy of the Santa Mera Mb. across these mesoscale extensional faults have been found, suggesting a certain control of faulting in the sedimentation of the Santa Mera Mb.

In addition, four fracture systems have been appreciated in the Buerres Mb. of the Conejera Fault hanging-wall block (*i.e.* joint sets 1, 2, 3 and faults). Once bedding is restored to the horizontal, it becomes clear that sets 1 and 2 are both mutually perpendicular as well as normal to bedding (Fig. 10). As revealed by our structural analysis, once rotated, these joint sets are neither parallel nor perpendicular to the NE-striking Conejera Fault and the other extensional faults in its footwall and hanging-wall. In the simplest plane

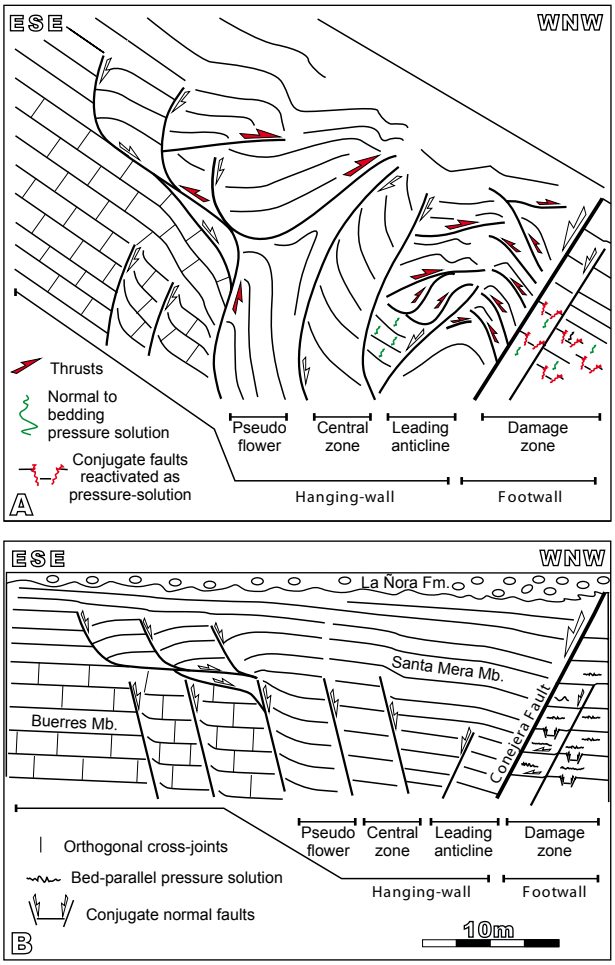

FIGURE 11. Conceptual restoration of the Conejera fault blocks. A) Present day structure. B) Once the post-extensional deformation is removed.

strain case scenario, the observed orthogonal cross-joint system deviates from a theoretically expected assemblage related to extension (*i.e.* one joint set normal to the main extensional faults, and one set parallel to them; Jaeger and Cook, 1979; Fossen, 2016). In addition, the joints are also folded by the drape folds developed above the extensional faults in the Conejera hanging-wall Buerres Mb. layers, thus, indicating that these joints pre-date layer titling and the extensional faulting. Careful observation also indicates that the hanging-wall NE-striking normal faults developed by linkage of this orthogonal cross-joint system too (Fig. 10E). These observations support a growth model from joints to sheared joints evolving into extensional faults (*e.g.* Wilkins *et al.*, 2001).

Contractional kinematics

The contractional deformation pattern in the Conejera fault blocks is represented by a system of contractional folds, thrusts and pressure solution seams with a

predominant NE to ENE trend (Figs. 11; 12). The normal stratigraphic separation observed for the Conejera Fault and the shortening distribution in the hanging-wall and footwall blocks indicate that the contractional reactivation of the Conejera Fault was limited or even not mechanically favourable. The described contractional deformation has been strongly controlled by: i) the mechanical stratigraphy contrasts between the upper and lower members of the Rodiles Fm. and ii) the inherited extensional architecture. The contractional deformation pattern is, therefore, broadly consistent with a buttressing deformation style (*e.g.* Butler, 1989). Upon shortening, folding of the multilayered Santa Mera Mb., development of footwall- and hanging-wall directed thrusts (McClay, 1989) and associated thrust-related folding took place (Fig. 12A). The Conejera Fault blocks also attained bulk strain close to the fault as indicated by pressure solution seams in both the hanging-wall and footwall. The orientation of this pressure solution is consistent with shortening parallel to bedding. In the footwall block, pressure solution was concentrated on the planes of previously developed conjugate extensional faults, as well in other planes normal to bedding (Fig. 5). The relationships between these reactivated faults, and solution seams and the footwall bedding suggest that pressure solution developed during the layer-parallel shortening prior to the northwards tilting of the footwall beds.

In the absence of fault plane striations on the Conejera Fault, the attitude of these pressure solution seams and the orientation of the compressive folds and thrusts in the hanging-wall can be used as a proxy for the direction of Alpine convergence. Lack of any remarkable strike-slip related structure within the studied fault zones, along with the substantial parallelism between the extensional faults and the contractional structures (Figs. 4; 5; 6), suggest

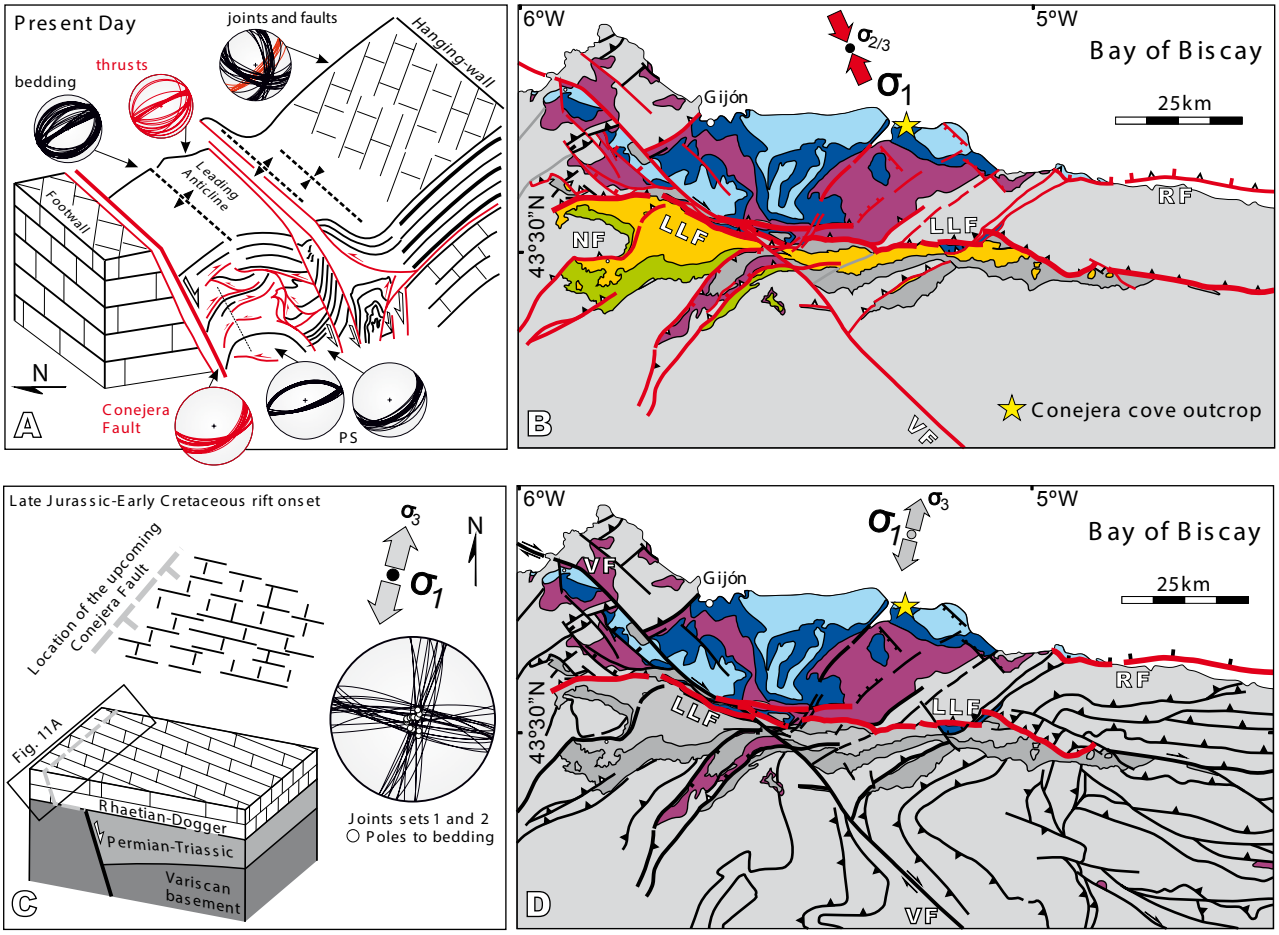

FIGURE 12. Discussion of results. A) 3D block diagram illustrating the structure and structural data orientation in the Conejera fault blocks. B) Main reactivated faults in the onshore Asturian Basin during Alpine convergence based on Lepvrier and Martínez-García (1990). Red arrows indicate the orientation of the main compressive principal stress (σ1) inferred from this study. See Figure 1 for the legend of map units. C) Trace map and 3D block diagram of the Conejera structure with joint and fault patterns at the onset of the Late Jurassic-Early Cretaceous rifting. Grey arrows indicate the remote regional paleo-stress related with this incipient rifting. D) Main Late Jurassic-Early Cretaceous extensional faults. Grey arrows indicate the direction of the least principal stress (σ3) related with the Late Jurassic-Early Cretaceous rifting. NF: Naranco Fault; RF: Ribadesella Fault; LLF: Llanera Fault; VF: Ventaniella Fault; PS: Pressure Solution.

that Alpine shortening could have been oriented at high angles to the NE-striking faults (Fig. 12B). However, the orientation of these contractional structures may also result from a local reorientation of the regional maximum compressive stress (*i.e.* σ1) near the pre-existing NE-striking Conejera Fault.

Regional contextualization

Normal offset across the Conejera Fault took place either in Middle Jurassic times, based on minor stratigraphic thickness changes in the Dogger series (Uzkeda *et al.*, 2013), or during the Upper Jurassic-Lower Cretaceous rifting episode (Valenzuela *et al.*, 1986; Lepvrier and Martínez-García, 1990). Although the relationships between the Kimmeridgian strata, the Lower-Middle Jurassic carbonates and the Conejera Fault are not fully exposed on the studied section, we favour the Upper Jurassic-Lower Cretaceous age for the main extensional movement based on its regional evidence. Unconformities revealed by seismic data in the offshore domain, indicate the onset of compressional deformation in the Asturian Basin as early as late Santonian (Upper Cretaceous) protracting until the Miocene (Riaza-Molina, 1996; Gallastegui, 2000; Ferrer *et al.*, 2008). Onshore, Alonso and Pulgar (2004) and De Vicente *et al.* (2007) indicated movement along NE-striking basement-involved faults during Alpine compression with both NW- and SE-directed reverse fault kinematics. The activity of some of these onshore basement-involved faults is dated as post lower Oligocene based on the ages of the overridden footwall strata (De Vicente *et al.*, 2007). Given the lack of a sedimentary record of these ages around the Conejera cove, the time of contractional deformation cannot be precisely determined.

One interesting outcome of our work comes from the hanging-wall pattern of joints. Joints are commonly used to decipher the orientation of the regional stress field, its temporal and spatial evolution (see Engelder and Geiser, 1980; Dyer, 1988; Olson and Pollard, 1989; Bai *et al.*, 2002). Given the here demonstrated relative-timing deformation pattern at Conejera cove, and the well-constrained timing of events in the Asturian Basin and Bay of Biscay (*e.g.* Sibuet *et al.*, 1971, 2007; Arthaud and Matte, 1977; Boillot, 1984; Valenzuela *et al.*, 1986; Dallmeyer and Martínez-García, 1990; Lepvrier and Martínez-García, 1990; Álvarez-Marron *et al.*, 1996; Gallastegui, 2000; Ferrer *et al.*, 2008; Roca *et al.*, 2011; Grobe *et al.*, 2014; Tugend *et al.*, 2014), the best plausible timing for the generation of the observed orthogonal cross-joint pattern (*i.e.* sets 1 and 2) should correspond to the incipient stages of Late Jurassic-Early Cretaceous rifting (Fig. 12 C). Once rotated, set 1 joints strike ESE-WNW (*i.e.* about N100E), almost parallel to the E-trending Asturian Basin axis and the main basin bounding faults (*i.e.* the onshore Llanera and Ribadesella faults), whereas the joint set 2 becomes roughly perpendicular to these faults (*i.e.* NNE-SSW; Fig. 12D). The presence of two perpendicular sets of joints striking about N015E and N100E allows defining the regional stretching direction. Because these two mutually perpendicular sets represent a classical orthogonal pattern, they can be interpreted as having developed in areas -or during periods- of negligible stress perturbation. Therefore these joints must have developed in the suprasalt sedimentary cover, prior to the reactivation of the underlying basement faults. Thus, the regional σ3 would have been parallel to the predominant N015E extensional fracture set, very similar to the stretching direction suggested by Tavani and Muñoz (2012) in the Basque-Cantabrian Basin (*i.e.* N020E). Given the scarcity of similar studies in the Asturian Basin, we compare here our results to previous mesostructural studies from other Late Jurassic-Early Cretaceous basins of North Iberia, such as the Basque-Cantabrian and the Cameros basins (Fig. 13). In this regard, Soto *et al.* (2008) and Oliva-Urcia *et al.* (2013) define by means of the AMS technique (*i.e.* Anisotropy of the Magnetic Susceptibility) a predominant NE- to N-stretching direction that they assign to the Late Jurassic-Early Cretaceous development of these basins, an interpretation that is in good agreement with that presented in this work.

The origin of the NNW-striking joints of set 3 remains speculative, though. Set 3 joints share a similar orientation to those reported by Uzkeda *et al.* (2016) for the Asturian Basin; they could be considered as belonging to the same fracture system as set 2 and constitute as well part of the abutting joints of the orthogonal cross-joint system. However, set 3 joints are not perfectly perpendicular to bedding nor to set 1 joints. For this reason, set 3 joints could correspond to: i) the same Late Jurassic-Early Cretaceous rifting, or ii) the early Alpine shortening which would have been parallel to this joint set, and, therefore, indicating a SSE-directed direction of shortening.

CONCLUSIONS

The studied structures at Conejera cove correspond to the Conejera Fault and its hanging-wall and footwall blocks. The Conejera Fault is a NE-striking cover extensional fault detached along the uppermost Triassic to lowermost Jurassic evaporites, and may have been kinematically-linked to a basement-involved fault located beneath these evaporites. Although the Conejera Fault displays an extensional offset, the observed structural styles and deformation patterns indicates that the hanging-wall and footwall blocks have undergone contractional deformation during Alpine shortening. Field observations and structural analysis have revealed as well

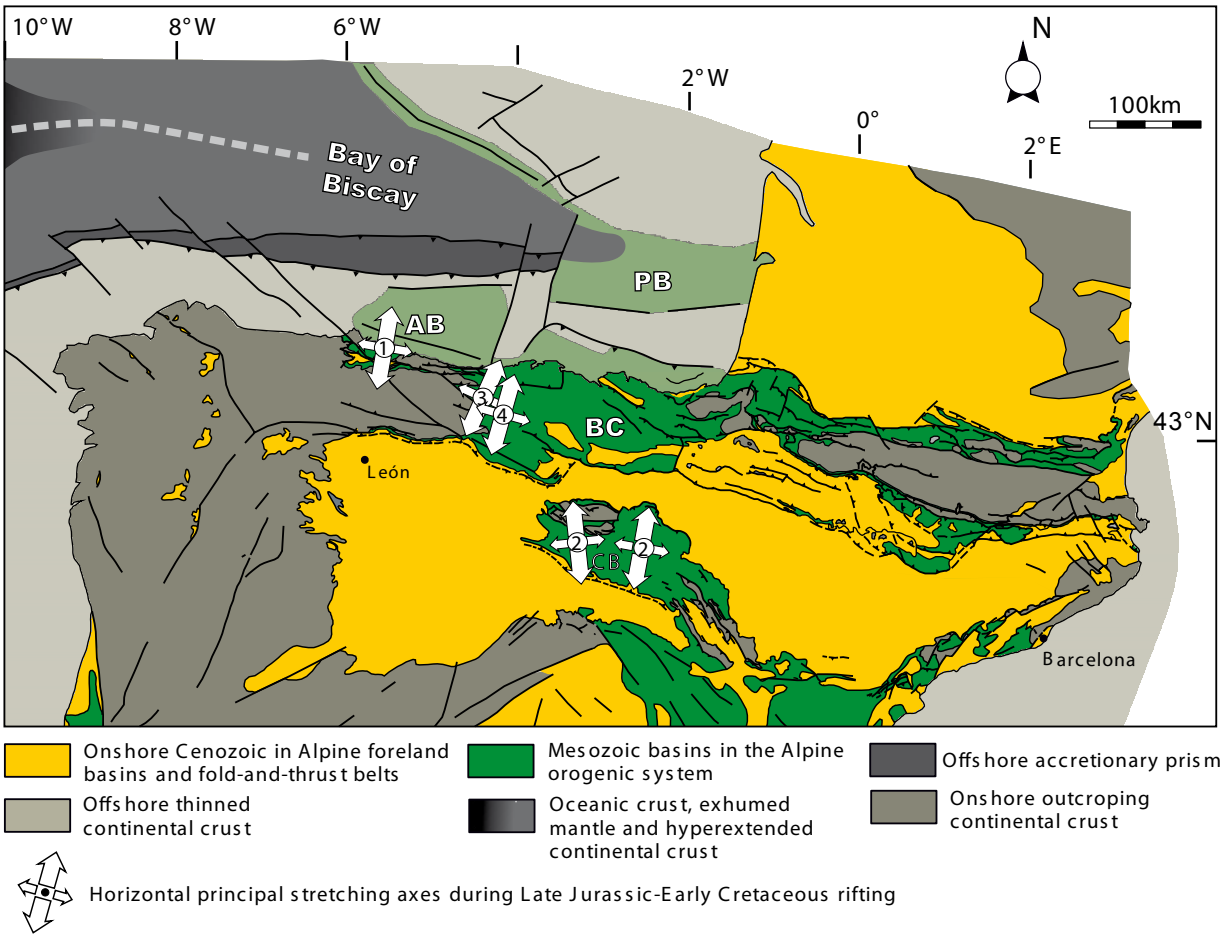

FIGURE 13. Location of main Late Jurassic-Early Cretaceous basins in northern Iberia and the adjoining Bay of Biscay. Arrows indicate the inferred directions and relative magnitude of the horizontal principal stresses. 1) This study; 2) Soto *et al.* (2008); 3) Oliva-Urcia *et al.* (2013); 4) Tavani and Muñoz (2012). Figure modified from Muñoz (2002) and Roca *et al.* (2011). AB: Asturian Basin; BCC: Basque-Cantabrian Basin; CB: Cameros Basin; PB: Parentis Basin.

that: i) onset of extensional faulting may have started as early as coeval to the sedimentation of the Santa Mera Mb. Such extensional architecture imposed a significant control on the subsequent compressional deformation, broadly decoupling deformation between the Santa Mera and the Buerres mbs., ii) a system of orthogonal cross-joints oblique to the Conejera Fault and other major onshore faults was developed in the incipient stages (*i.e.* pre-faulting) of Late Jurassic-Early Cretaceous rifting as a response to the remote stretching stress field, iii) a second system of meso-extensional faults parallel to the Conejera Fault was subsequently developed by the reactivation and linkage of the orthogonal cross-joints system, iv) a system of contractional folds, thrusts and pressure solution seams with a predominant NE to ENE trend was developed during the following shortening phase, v) an obliquity between the here inferred direction of Late Jurassic-Early Cretaceous stretching (*i.e.* about N015E) and the onshore boundary faults of the Asturian Basin is indicated. The contractional structures are broadly parallel to the NE-striking Conejera Fault and suggest a roughly SSE- to SE-oriented Alpine convergence.

ACKNOWLEDGMENTS

Earlier versions of this article benefited from the suggestions and comments of two anonymous reviewers and the editors. We want to express our gratitude for the invitation to contribute to this special volume in honour of Prof. P. Santanach (University of Barcelona). This is a contribution of the Institut de Recerca Geomodels and the Geodinàmica i Analisi de Conques research group (2014SGR467SGR), from the Agència de Gestió d'Ajuts Universitaris i de Recerca (AGAUR) and the Secretaria d'Universitats i Recerca del Departament d'Economia i Coneixement de la Generalitat de Catalunya.

REFERENCES

Agosta, F., Aydin, A., 2006. Architecture and deformation mechanism of a basin-bounding normal fault in Mesozoic platform carbonates, central Italy. Journal of Structural Geology, 28, 1445-1467.

Alonso, J.L., Pulgar, J.A., García-Ramos, J.C., Barba, P., 1996. Tertiary Basins and Alpine Tectonics in the Cantabrian Mountains. In: Friend, P.F., Dabrio, C.J. (eds.). Tertiary Basins of Spain: the stratigraphic record of crustal kinematics. Cambridge, University Press, 214-227.

Alonso, J.L., Pulgar, J.A., 2004. Estructura alpina de la Cordillera Cantábrica: generalidades. En: Vera, JA. (ed.). Geología de España. Madrid, SGE-IGME, 332-343.

Alonso, J.L., Martínez Abad, I., García Ramos, J.C., 2007. Nota sobre la presencia de una sucesión cretácica en el Macizo de Las Ubiñas (Cordillera Cantábrica). Implicaciones tectónicas y geomorfológicas. Geogaceta, 43, 47-50.

Álvarez-Marrón, J., Pérez-Estaún, A., Dañobeitia, J.J., Pulgar, J.A., Martínez Catalán, J.R., Marcos, A., Bastida, F., Ayarza Arribas, P., Aller, J., Gallart, J., González-Lodeiro, F., Banda, E., Comas, M.C., Córdoba, D., 1996. Seismic structure of the northern continental margin of Spain from ESCIN deep seismic profiles. Tectonophysics, 264, 153-174.

Arthaud, F., Matte, Ph., 1977. Late Paleozoic strike-slip faulting in southern Europe and northern Africa: result of a right-lateral shear zone between the Appalachians and the Urals. Bulletin Geological Society America, 88, 1305-1320.

Barrón, E., Gómez, J.J., Goy, A., Pieren, A.P., 2006. The Triassic-Jurassic boundary in Asturias (northern Spain): Palynological characterization and facies. Review of Palaeobotany and Palynology, 138, 187-208.

Bai, T., Maerten, L., Gross, M.R., Aydin, A., 2002. Orthogonal cross joints: do they imply a regional stress rotation? Journal of Structural Geology, 24, 77 -88.

Bergbauer, S., Pollard, D.D., 2004. A new conceptual fold-fracture model including prefolding joints, based on the Emigrant Gap anticline, Wyoming. Geological Society of America Bulletin, 116, 294-307.

Blenkinsop, T.G., 2008. Relationships between faults, extension fractures and veins, and stress. Journal of Structural Geology, 30, 622-632.

Boillot, G., 1984. Le Golfe de Gascogne et les Pyrénées. In: Boillot, G. (ed.). Lesmarges continentales actuelles et fossiles autour de la France. Paris, Masson, 5-81.

Boillot, G., Dupeuble, P.A., Malod, J., 1979. Subduction and tectonics on the continental margin of northern Spain. Marine Geology, 32, 53-70.

Boyer, S.E., 1995. Sedimentary basin taper as a factor controlling the geometry and advance of thrust belts. American Journal of Science, 295, 1220-1254.

Brogi, A., 2011. Variation in fracture patterns in damage zones related to strike-slip faults interfering with pre-existing fractures in sandstone (Calcione area, southern Tuscany, Italy). Journal of Structural Geology, 33, 644-661.

Butler, R.W.H., 1989. The influence of pre-existing basin structure on thrust system evolution in the western Alps. In: Cooper, M.A., Williams, G.D. (eds.). Inversion Tectonics. Geological Society, Special Publication, 44, 105-122.

Butler, R.W.H., Tavarnelli, E., Grasso, M., 2006. Structural inheritance in mountain belts: an Alpine-Apennine perspective. Journal of Structural Geology, 28, 1893-1908.

Cadenas, P., Fernández-Viejo, G., 2017. The Asturian Basin within the North Iberian margin (Bay of Biscay): seismic characterisation of its geometry and its Mesozoic and Cenozoic cover. Basin Research, 29, 521-541. DOI: 10.1111/bre.12187

Carola, E. Tavani, S., Ferrer, O., Granado, P., Quintà, A., Butillé, M., Muñoz, J.A., 2013. Along-strike extrusion at the transition between thin- and thick-skinned domains in the Pyrenean Orogen (northern Spain). In: Nemok, N., Mora, A., Cosgrove, J. (eds.). Thick-skin-dominated orogens; from initial inversion to full accretion. Geological Society, Special Publications, 377, 119-140.

Carrera, N., Muñoz, J.A., Sàbat, F., Mon, R., Roca, E., 2006. Role of inversion tectonics in the structure of the Cordillera Oriental (NW Argentinean Andes). Journal of Structural Geology, 28, 1921-1932.

Cooper, M.A., Williams, G.D., 1989. Inversion Tectonics. Geological Society of London, Special Publication, 44, 275-308.

Coward, M.P., Enfield, M.A., Fischer, M.W., 1989. Devonian basins of Northern Scotland: extension and inversion related to Late Caledonian-Variscan tectonics. In: Cooper, M.A., Williams, G.D. (eds.). Inversion Tectonics. Geological Society of London, Special Publication, 44, 275-308.

Coward, M.P., Gillcrist, R., Trudgill, B., 1991. Extensional structures and their tectonic inversion in the Western Alps. In: Roberts, A.M., Yielding, G., Freeman, B. (eds.), The Geometry of Normal Faults. Geological Society of London, Special Publication, 56, 93-113.

Crider, J.G., Peacock, D.C.P., 2004. Initiation of brittle faults in the upper crust: a review of field observations. Journal of Structural Geology, 26, 691-707.

Cruikshank, K.M., Zhao, J., Johnson, A.M., 1991. Analysis of minor fractures associated with joints and faulted joints. Journal of Structural Geology, 13, 865-886.

Dallmeyer, R.D., Martínez-García, E., 1990. Pre-Mesozoic Geology of Iberia. IGCP Project 233. Berlin Heidelberg, Springer-Verlag, 416pp.

Davis, D.M., Engelder, T., 1985. The role of salt in fold and thrust belts. Tectonophysics, 119, 67-88.

De Gracianski, P.C., Dardeau, G., Lemoine, M., Tricat, P., 1989. The inverted margin of the French Alps and foreland basin inversion. In: Cooper, M.A., Williams, G.D. (eds.). Inversion Tectonics. Geological Society of London, Special Publications, 44, 87-104.

De Vicente, G., González-Nistal,S., Muñoz-Martín, A., Vegas, R., Olaiz, A., Fernández-Lozano, J., De Vicente, R., 2007. El cabalgamiento cenozoico de Boinás (Cordillera Cantábrica, España). Geogaceta, 42, 7-10.

Dyer, R., 1988. Using joint interactions to estimate paleostress ratios. Journal of Structural Geology, 10, 685-699.

Engelder, T., Geiser, P.A., 1980. On the use of regional joint sets as trajectories of paleostress fields during the development of the Appalachian Plateau. Journal of Geophysical Research, 85, 6319-6341.

Ferrer, O., Roca, E., Benjumea, B., Muñoz, J.A., Ellouz, N., MARCONI Team, 2008. The deep seismic reflection MARCONI-3 profile: Role of extensional Mesozoic structure during the Pyrenean contractional deformation at the eastern part of the Bay of Biscay. Marine and Petroleum Geology, 25, 714-730.

Fossen, H., 2016. Structural Geology. Cambridge, Cambridge University Press, 510pp.

Frizon de Lamotte, D., Leturmy, P-., Missenard, Y., Khomsi, S., Ruiz, G., Saddiqi, O., Guillocheau, F., Michard, A., 2009. Mesozoic and Cenozoic vertical movements in the Atlas system (Algeria, Morocco, Tunisia): An overview. Tectonophysics, 475, 9-28.

Gallastegui, J., Pulgar, J.A., Álvarez-Marrón, J., 1997. 2-D seismic modelling of the Variscan foreland thrust and fold belt crust in NW Spain from ESCIN-1 deep seismic reflection data. Tectonophysics, 269, 21-32.

Gallastegui, J., 2000. Estructura cortical de la Cordillera y Margen Continental Cantábricos: Perfiles ESCI-N. PhD Thesis. Oviedo, Universidad de Oviedo (España). Trabajos de Geología, 22, 234pp.

Gillcrist, R., Coward, M.P.A., Mugnier, J.L., 1987. Structural inversion and its controls: examples from the Alpine foreland and the French Alps. Geodinamica Acta, 1, 5-34.

Graham Wall, B., Antonellini, M., Aydin, A., 2003. Formation and growth of normal faults in carbonates within a compressive environment. Geology, 31, 11-14.

Granado, P., Thöny, W., Carrera, N., Grazter, P., Strauss, P., Muñoz, J.A., 2016. Basement-involved reactivation in foreland fold and thrust belts: the Alpine-Carpathian Junction (Austria). Geological Magazine, 153 (5-6), 1110-1035.

Granado, P., Ferrer, O., Muñoz, J.A., Thöny, W., Strauss, P., 2017. Basin inversion in tectonic wedges: Insights from analogue modelling and the Alpine-Carpathian fold-and-thrust belt. Tectonophysics, 703-704, 50-68.

Grobe, R.W., Álvarez-Marrón, J., Glasmacher, U.A., Stuart, F.M., 2014. Mesozoic exhumation history and palaeolandscape of the Iberian Massif in eastern Galicia from apatite fission-track and (U+Th)/He data. International Journal of Earth Science, 103, 539-561.

Gross, M.R., 1993. The origin and spacing of cross joints: examples from the Monterey Formation, Santa Barbara Coastline, California. Journal of Structural Geology, 15, 737-751.

Hardy, S., McClay, K., 1999. Kinematic modelling of extensional fault propagation folding. Journal of Structural Geology, 21, 695-702.

Henza, A.A., Withkack, M.O., Schlische, R.W., 2011. How do properties of a pre-existing normal-fault population influence fault development during a subsequent phase of extension? Journal of Structural Geology, 33, 1312-1324.

Hillis, E.S., 1956. A contribution to the morphotectonics of Australia. Journal of the Geological Society of Australia, 3, 1-15.

Jackson, C.A.L., Gawthorpe, R.L., Sharp, I.R., 2006. Style and sequence of deformation during extensional fault-propagation folding: examples from the Hammam Faraun and El-Qaa fault blocks, Suez Rift, Egypt. Journal Structural Geology, 28, 519-535.

Jaeger, G.D., Cook, N.G.W., 1979. Fundamentals of Rock Mechanics. London, Chapman and Hill Ltd., 515pp.

Lepvrier, C., Martínez-García, E., 1990. Fault development and stress evolution of the post-Hercynian Asturian Basin (Asturias and Cantabria, northwest Spain). Tectonophysics, 184, 345-356.

Macedo, J.M., Marshack, S., 1999. Controls on the geometry of fold-thrust belt salients. Geological Society of America Bulletin, 111, 1808-1822.

McClay, K.R., 1989. Analogue models of inversion tectonics. In: Cooper, M.A., Williams, G.D. (eds.), Inversion Tectonics. Geological Society of London, Special Publication, 44, 41-59.

McClay, K.R., 1995. The geometries and kinematics of inverted fault systems: a review of analogue model studies. In: Buchanan, J.G., Buchanan, P.G. (eds.). Basin Inversion. Geological Society of London, Special Publication, 88, 97-118.

Muñoz, J.A., 2002. The Pyrenees. In: Gibbons, W. Moreno, M.T. (eds.). The Geology of Spain. Geological Society of London, 370-385.

Myers, R., Aydin, A., 2004. The evolution of faults formed by shearing across joint zones in sandstone. Journal of Structural Geology, 26, 947-966.

Olson, J.E., Pollard, D.D., 1989. Inferring paleostress from natural fracture patterns: a new method. Geology, 17, 345-348.

Oliva-Urcia, B., Román-Berdiel, T., Casas, A.M., Bógalo, M.F., Osácar, M.C., García-Lasanta, C., 2013. Transition from extensional to compressional magnetic fabrics in the Cretaceous Cabuérniga basin (North Spain). Journal of Structural Geology, 46, 220-234.

Pignatelli, R., Giannini, G., Ramírez del Pozo, J., Beroiz, C., Barón, A., 1973. Mapa Geológico de España, 1:50.000, serie magna, hoja 15 (Lastres). Madrid, Instituto Geológico y Minero de España, 25pp.

Pulgar, J.A., Alonso, J.A., Espina, R.G., Marin, J.A., 1999. La deformación alpina en el basamento varisco de la Zona Cantábrica. Trabajos de Geología, 21, 283-294.

Riaza-Molina, C., 1996. Inversión estructural en la cuenca mesozoica del offshore asturiano. Revisión de un modelo exploratorio. Geogaceta, 20, 169-171.

Robles, S., Quesada, S., Rosales, I., Aurell, M., García-Ramos, J.C., 2004. El Jurásico marino de la Cordillera Cantábrica. In: Geología de España. Madrid, Sociedad Geológica de España-Instituto Geológico y Minero de España, 279-281.

Roca, E., Muñoz, J.A., Ferrer, O., Ellouz, N., 2011. The role of the Bay of Biscay Mesozoic extensional structure in the configuration of the Pyrenean orogen: constrains from the MARCONI deep seismic reflection survey. Tectonics, 30 TC2001 2011. DOI: 10.1029/2010TC002735

Schlische, R.W., 1995. Geometry and origin of fault-related folds in extensional settings. American Association of Petroleum Geologists Bulletin, 79, 1661-1678.

Schudack, M., Schudack, U., 2002. New biostratigraphical data from the Upper Jurassic of Asturias (Northern Spain) based on Ostracoda. Revista Española de Micropaleontología, 34, 1-18.

Sibuet, J.C., Pautot, G., Le Pichon, X., 1971. Interpretation structurale du golfe de Gascogne à partir des profiles de sismique. In: Debyser, J., Le Pichon, Montadert, L. (eds.). Histoire Structurale du Golfe de Gascogne. Publications de l'Institut Français du Pétrole, 22, 6(10), 1-31.

Sibuet, J.C., Srivastava, S., Manatschal, G., 2007. Exhumed mantle-forming transitional crust in the Newfoundland-Iberia rift and associated magnetic anomalies, Journal of Geophysical Research, 112, B06105. DOI: 10.1029/2005JB003856

Silliphant, L.J., Engelder, T., Gross, M.R., 2002. The state of stress in the limb of the Split Mountain anticline, Utah: constrains placed by transected joints. Journal of Structural Geology, 24, 155-172.

Soto, R., Casas-Sainz, A.M., Villalain, J.J., Gil-Imaz, A., Fernández-González, G., Del Río, P., Calvo, M., Mochales, T., 2008. Characterizing the Mesozoic extension direction in the northern Iberian Plate margin by anisotropy of magnetic susceptibility (AMS). Journal of the Geological Society of London, 165, 1007-1018.

Suárez-Vega, L.C., 1974. Estratigrafía del Jurásico de Asturias. Cuadernos de Geología Ibérica, 74, 1-369.

Tavani, S., Quintà, A., Granado, P., 2011a. Cenozoic right-lateral wrench tectonics in the Western Pyrenees (Spain): The Ubierna Fault System. Tectonophysics, 509, 238-253.

Tavani, S., Mencos, J., Bausà, J., Muñoz, J.A., 2011b. The fracture pattern of the Sant Corneli-Bóixols oblique inversion anticline (Spanish Pyrenees). Journal of Structural Geology, 33, 1662-1680.

Tavani, S., Muñoz, J.A., 2012. Mesozoic rifting in the Basque–Cantabrian Basin (Spain): Inherited faults, transversal structures and stress perturbation. Terra Nova, 24, 70-76.

Tavani, S., Carola, E., Granado, P., Quintà, A., Muñoz, J.A., 2013. Transpressive inversion of a Mesozoic extensional forced fold system with an intermediate décollement level in the Basque-Cantabrian Basin (Spain). Tectonics, 32, 146-158.

Tavani, S., Granado, P., 2015. Along-strike evolution of folding, stretching and breaching of supra-salt strata in the Plataforma Burgalesa extensional forced fold system (northern Spain). Basin Research, 27, 573-585.

Tavarnelli, E., 1996. Tethyan heritage in the development of the Neogene Umbria-Marche fold-and-thrust belt, Italy: a 3D approach. Terra Nova, 8, 470-478.

Thomas, D.W., Coward, M.P., 1995. Upper Jurassic-Early Cretaceous inversion of the northern East Shetland Basin, northern North Sea. In: Buchanan, J.G., Buchanan, P.G. (eds.). Basin inversion. Geological Society of London, Special Publication, 88, 275-306.

Tugend, J., Manatschal, G., Kusznir, N.J., Masini, E., Mohn, G., Thinon, I, 2014. Formation and deformation of hyperextended rift systems: Insights from rift domain mapping in the Bay of Biscay-Pyrenees. Tectonics, 33, 1239-1276. DOI: 10.1002/2014TC003529

Turner, J.P., Williams, G.A., 2004. Basin inversion and intra-plate shortening. Earth-Science Reviews, 65, 277-304.

Uzkeda, H., Bulnes, M., Poblet, J., García-Ramos, J.C., Piñuela, L., 2013. Buttressing and reverse reactivation of a normal fault in Jurassic rocks of the Asturian Basin, NW Iberian Peninsula. Tectonophysics, 599, 117-134.

Uzkeda, H., Bulnes, M., Poblet, J., García-Ramos, J.C., Piñuela, L., 2016. Jurassic extensión and Cenozoic inversion tectonics in the Asturian Basin, NW Iberian Peninsula: 3D structural model and kinematic evolution. Journal of Structural Geology, 90, 157-176.

Valenzuela, M., García-Ramos, J.C., Suárez de Centi, C., 1986. The Jurassic sedimentation in Asturias (N Spain). Trabajos de Geología, 16, 121-132.

White, S.H., Bretan, P.G., Rutter, E.H., 1986. Fault-zone reactivation: kinematics and mechanisms. Philosophical Transactions of the Royal Society, London, A317, 81-97.

Wilkins, S.J., Gross, M.R., Wacker, M., Eyal, Y., Egelder, T., 2001. Faulted joints: kinematics, displacement-length scaling relations and criteria for their identification. Journal of Structural Geology, 23, 315-327.

Willemse, E.J.M., Peacock, D.C.P., Aydin, A., 1997. Nucleation and growth of strike-slip faults in limestones from Somerset, U.K. Journal of Structural Geology, 19, 1461-1477.

Williams, G.D., Powell, C.M., Cooper, M.A., 1989. Geometry and kinematics of inversion tectonics. In: Cooper, M.A., Williams, G.D. (eds.). Inversion Tectonics. Geological Society of London, Special Publication, 44, 3-15.

Wilson, P., Gawthorpe, R.L., Hodgetts, D., Rarity, F., Sharp, I.R., 2009. Geometry and architecture of faults in a syn-rift fault array: The Nukhul half graben, Suez rift, Egypt. Journal of Structural Geology, 31, 759-775.

Zamora, G., Fleming, M., Gallastegui, J., 2017. Salt tectonics within the offshore Asturian Basin: North Iberian Margin. In: Soto, J.I., Flinch, J.F., Tari, G. (eds.), Permo-Triassic salt provinces of Europe, North Africa and the Atlantic Margins. Tectonics and hydrocarbon potential. Part III, Atlantic Margins. Amsterdam, Elsevier, 353-367.

Manuscript received September 2017;
revision accepted February 2018;
published Online July 2018.